The EMBO Journal Vol.16 No.21 pp.6355–6363, 1997

Interferon action and apoptosis are defective in mice devoid of 2′,5′-oligoadenylate-dependent RNase L

Aimin Zhou[1,2], Jayashree Paranjape[1], Thomas L.Brown[3], Huiqin Nie[1], Sharon Naik[1], Beihua Dong[1], Ansi Chang[4], Bruce Trapp[4], Robert Fairchild[5], Clemencia Colmenares[1] and Robert H.Silverman[1,2,6]

[1]Departments of Cancer Biology, [3]Cell Biology, [4]Neurosciences and [5]Immunology, The Lerner Research Institute, The Cleveland Clinic Foundation, Cleveland, OH 44195 and [2]The Department of Chemistry, Cleveland State University, Cleveland, OH 44115, USA

[6]Corresponding author

2′,5′-Oligoadenylate-dependent RNase L functions in the interferon-inducible, RNA decay pathway known as the 2-5A system. To determine the physiological roles of the 2-5A system, mice were generated with a targeted disruption of the RNase L gene. The antiviral effect of interferon α was impaired in RNase L$^{-/-}$ mice providing the first evidence that the 2-5A system functions as an antiviral pathway in animals. In addition, remarkably enlarged thymuses in the RNase L$^{-/-}$ mice resulted from a suppression of apoptosis. There was a 2-fold decrease in apoptosis *in vivo* in the thymuses and spleens of RNase L$^{-/-}$ mice. Furthermore, apoptosis was substantially suppressed in RNase L$^{-/-}$ thymocytes and fibroblasts treated with different apoptotic agents. These results suggest that both interferon action and apoptosis can be controlled at the level of RNA stability by RNase L. Another implication is that the 2-5A system is likely to contribute to the antiviral activity of interferon by inducing apoptosis of infected cells.

Keywords: 2-5A/apoptosis/interferon/RNase L/virus

Introduction

The 2-5A system is a regulated RNA decay pathway induced by interferon treatment of mammalian cells (Kerr and Brown, 1978). Involvement of the 2-5A system in some of the antiviral and anticellular proliferation effects of interferon has been inferred from results of cell culture experiments (Williams *et al.*, 1979; Hassel *et al.*, 1993). For instance, the 2-5A system has been suggested to function in antiviral effects of interferon against encephalomyocarditis virus (EMCV), reovirus and vaccinia virus (reviewed in Silverman and Cirino, 1997). The proposed molecular mechanism involves activation of a cellular endoribonuclease resulting in the degradation of both viral and cellular RNA. However, evidence for the antiviral function of the 2-5A system in animals has been lacking.

The effects of the 2-5A system are mediated by the 2′,5′-oligoadenylate-dependent endoribonuclease, RNase L, a uniquely regulated enzyme (Silverman, 1997). To catalyze the cleavage of single-stranded RNA, RNase L requires activators consisting of unusual, short 2′,5′-linked oligoadenylates (2-5A) with the formula $p_xA(2'p5'A)_y$, $x = 1$ to 3, $y = 2$ to $\geqslant 4$ (Kerr and Brown, 1978). 2-5A is produced from ATP by several isozymes of 2-5A synthetase, dsRNA-dependent enzymes that occupy different intracellular compartments (Chebath *et al.*, 1987a; Rutherford *et al.*, 1991). Cellular levels of both RNase L and the 2-5A synthetases are increased after interferon treatment (Hovanessian *et al.*, 1977; Jacobsen *et al.*, 1983). 2-5A induces dimerization of RNase L while converting the silent form of the enzyme into a potent ribonuclease (Dong *et al.*, 1994; Dong and Silverman, 1995; Cole *et al.*, 1996).

A more general role for RNase L beyond interferon action is suggested by its presence in nearly all mammalian cell types and organs from mouse to man (Silverman, 1997). In addition, enhanced levels of 2-5A synthetase or 2-5A *per se* were observed in chick oviducts induced to regress by withdrawal of estrogen stimulation and in rat mammary glands after cessation of lactation (Stark *et al.*, 1979; Reid *et al.*, 1984; Cohrs *et al.*, 1988). These studies suggested that the 2-5A system could, in some circumstances, cause RNA decay during cell death. Because cell death can limit viral spread in an organism, it is also possible that the 2-5A system exerts an *in vivo* antiviral activity by causing death of infected cells.

Host responses to viral infections include cell death by apoptosis (Vaux and Strasser, 1996). Identification of the enzymes that control and mediate the apoptotic process have led to elucidation of some of the molecular events. In particular, study of the caspase superfamily members and their inhibitors and of the bcl-2 family of apoptosis regulators has led to considerable insight into the apoptotic cell (Nagata, 1997). In contrast, definitive evidence for the participation and requirement of specific nucleases in the apoptotic process has been less obvious. A major limitation has been the absence of mice containing targeted disruptions in genes encoding nucleases involved in apoptosis. Indeed, the clearest evidence for involvement of specific proteins in biological processes, including apoptosis, is often provided by mutations that lead to a loss of protein and function. Therefore, to establish the physiological functions of the 2-5A system we have generated RNase L$^{-/-}$ mice. The absence of RNase L *in vivo* causes both a deficiency in the antiviral activity of interferon and a major defect in apoptosis. These findings, which implicate RNase L as a cell death factor, suggest both interferon action and apoptosis can be regulated at the level of RNA stability.

Results

A targeted insertion in the RNase L gene resulted in mice devoid of RNase L

To generate mice lacking a functional 2-5A system, a targeting vector was constructed in which a *neo* gene was

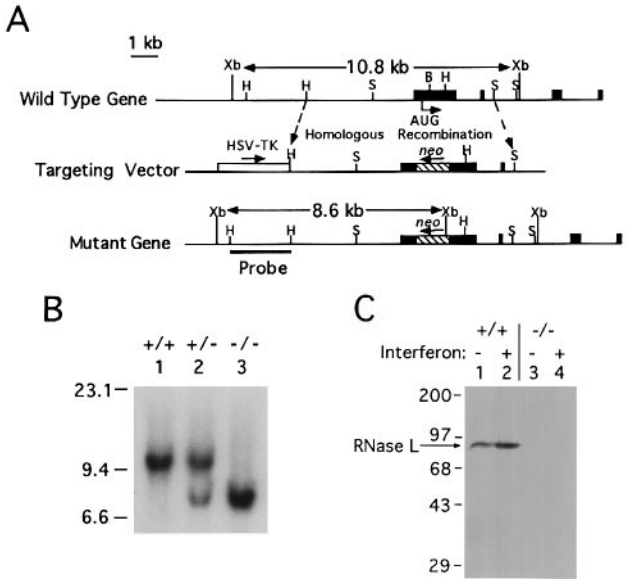

Fig. 1. Targeted disruption of the RNase L gene produces mice devoid of RNase L. (**A**) Map of the wild type RNase L gene, the targeting vector and the mutant RNase L gene. The coding exons are indicated by the closed boxes. The HSV TK gene is shown as an open box and the *neo* gene as a hatched box. The probe is indicated as a thick black line. Xb, *Xba*I; H, *Hin*dIII, S, *Sac*I. (**B**) Southern blot analysis of *Xba*I-digested DNA isolated from tails of wild type (lane 1), heterozygous (lane 2) and RNase $L^{-/-}$ (lane 3) mice. The probe was the *Hin*dIII/*Hin*dIII RNase L gene fragment shown in (A). (**C**) Absence of RNase L in primary MEF cells from RNase $L^{-/-}$ embryos determined on a Western blot probed with anti-RNase L antibody. MEF cells were incubated in the presence or absence of 1000 units/ml of interferon α as indicated.

inserted in reverse orientation into an RNase L gene fragment. The first coding exon of the murine RNase L gene encodes amino acids 1 to 491, 66% of the entire coding sequence. The *neo* insertion was in codon number 100 of the RNase L gene and, in addition, an HSV thymidine kinase gene was linked to the 5′-terminus of the RNase L gene fragment (Figure 1A). Amino acid residue 100 maps to the region of RNase L essential for 2-5A-binding activity (Zhou *et al.*, 1993). RNase L mutants missing 90 to 123 N-terminal amino acids were completely lacking in ribonuclease activity when incubated in either the presence or absence of 2-5A (Dong and Silverman, 1997). Therefore, the targeted disruption was designed to prevent the synthesis of a functional ribonuclease. After electroporation of the targeting construct into embryonic stem (ES) cells followed by positive/negative selection, two out of 230 $G418^R$, $ganciclovir^R$ clones contained a disrupted RNase L gene as determined by Southern blot analysis (for example see analysis of tail DNA in Figure 1B). The parental DNA produced a 10.8 kb fragment after digestion with *Xba*I and hybridization to an RNase L genomic DNA probe mapping outside the region of recombination. In contrast, DNA from cells containing the targeted insertion in the RNase L gene produced an additional band of 8.6 kb after *Xba*I digestion which hybridized both to the RNase L genomic probe and to a *neo* DNA probe (Figure 1A and B and not shown). After injection into blastocysts and implantation into foster mother mice, only one of the two clonal cell lines, AZ16, led to heterozygous mice with the disrupted RNase L gene in the germ line (Figure 1B, lane 2). Intercrosses of heterozygous mice produced homozygous, RNase $L^{-/-}$ mice at the expected frequency of approximately 1 in 4 (Figure 1B, lane 3). The RNase $L^{-/-}$ mice were fertile in intercrosses and the young offspring appeared normal.

To establish an absence of RNase L in the mice, Western blots of protein extracted from mouse embryo fibroblasts (MEF) lines, from RNase $L^{-/-}$ or wild type sibling embryos, were probed with a polyclonal antibody against murine RNase L. The fibroblasts were pretreated for 16 h with 1000 units/ml of interferon α to enhance levels of RNase L in the wild type cells. RNase L was clearly detected in the wild type cells and was enhanced by interferon treatment of the cells (Figure 1C, lanes 1 and 2). In contrast, RNase L could not be detected in the RNase $L^{-/-}$ cells regardless of the presence or absence of interferon treatment of the cells (lanes 3 and 4). To monitor further RNase L in the mice, extracts of several different organs were incubated with a high specific activity, ^{32}P-labeled and bromine-substituted 2-5A analog, $p(A2'p)_2(br^8A2'p)_2$-$A[^{32}P]Cp$ (Nolan-Sorden *et al.*, 1990). Upon irradiation with UV light at 308 nm, the 2-5A analog was covalently crosslinked to RNase L in extracts of seven different organs of the wild type mice (Figure 2A, lanes 1 to 7). The highest levels of RNase L were found in the spleen, thymus, lung and testis with lesser amounts in the kidney, liver and heart. The 2-5A binding proteins which appear smaller than RNase L may be degradation products of RNase L. In contrast, no RNase L or 2-5A binding proteins were found in extracts of organs of the RNase $L^{-/-}$ mice (lanes 8 to 14). To determine if any residual ribonuclease activity was present in the mutant mice, we transfected the 2-5A molecule, $p_3A(2'p5'A)_2$, into interferon treated primary MEF cells and determined the integrity of the 18S rRNA in Northern blots (Figure 2B) (Wreschner *et al.*, 1981; Silverman *et al.*, 1983). In wild type cells, the inactive nonphosphorylated core of 2-5A, $A(2'p5'A)_2$, did not cause cleavage of the rRNA whereas functional 2-5A, $p_3A(2'p5'A)_2$, produced the characteristic cleavage product (Figure 2B, lanes 2 and 3, respectively, see arrow). In contrast, there was no detectable degradation of the 18S rRNA in the interferon-treated RNase $L^{-/-}$ cells regardless of the presence or absence of $A(2'p5'A)_2$ or $p_3A(2'p5'A)_2$ (Figure 2B, lanes 4 to 6). These results demonstrate that RNase L is absent in the mutant mice.

The antiviral effect of interferon is suppressed in RNase $L^{-/-}$ cells and mice

To determine the effect of RNase L on replication of EMCV in cultured cells, wild type and RNase $L^{-/-}$ MEF cell lines were preincubated in the absence or presence of interferon α, infected with EMCV at a multiplicity of infection (MOI) of 0.01 plaque forming units (p.f.u.) per cell and incubated for two viral replication cycles (14 h). The interferon treatments resulted in dose-dependent decreases in viral yields in both the wild type and RNase $L^{-/-}$ cells (Figure 3A). However, with 0, 100 or 10 000 units/ml of added interferon there were 4-, 6- and 8-fold higher levels of virus produced in RNase $L^{-/-}$ cells compared with wild type cells. At a higher MOI (0.1), the differences between the cell lines were reduced (data not shown). These findings show that EMCV replicates

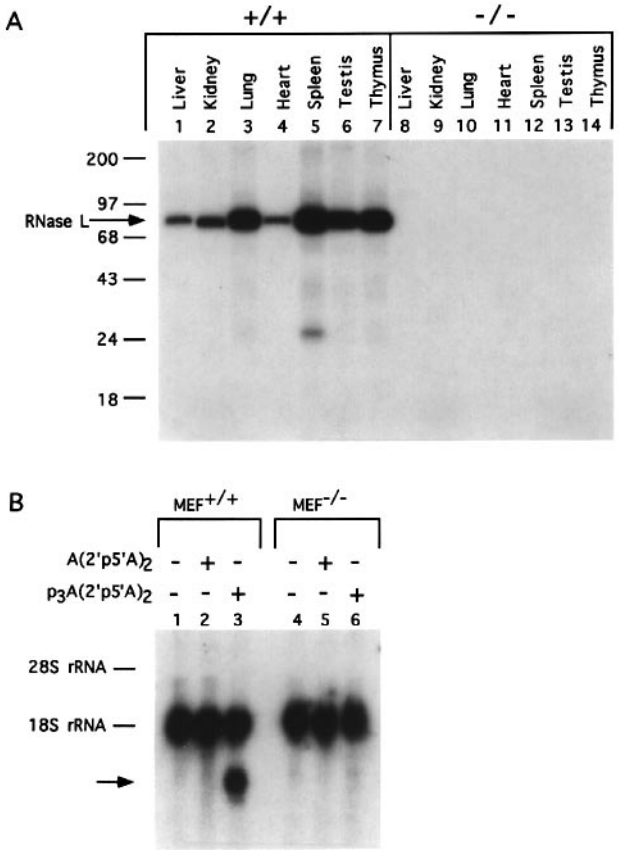

Fig. 2. 2-5A binding activity and RNase L activity are absent in RNase $L^{-/-}$ mice. (**A**) 2-5A binding assays were performed by UV covalent crosslinking of a ^{32}P-labeled 2-5A probe to RNase L. An autoradiogram of a dried SDS–polyacrylamide gel is shown of 2-5A binding assays performed with organ extracts of wild type mice (lanes 1–7) and RNase $L^{-/-}$ mice (lanes 8 to 14). (**B**) RNase L activity assays against 18S rRNA in intact cells. Wild type (lanes 1 to 3) or RNase $L^{-/-}$ (lanes 4 to 6) MEF cells were either mock transfect (lanes 1 and 4) or were transfected with inactive core 2-5A, $A(2'p5'A)_2$ (lanes 2 and 5) or with functional 2-5A, $p_3A(2'p5'A)_2$ (lanes 3 and 6). A Northern blot of the total RNA is shown probed with cDNA to 18S rRNA. The 18S rRNA cleavage product is indicated (arrow).

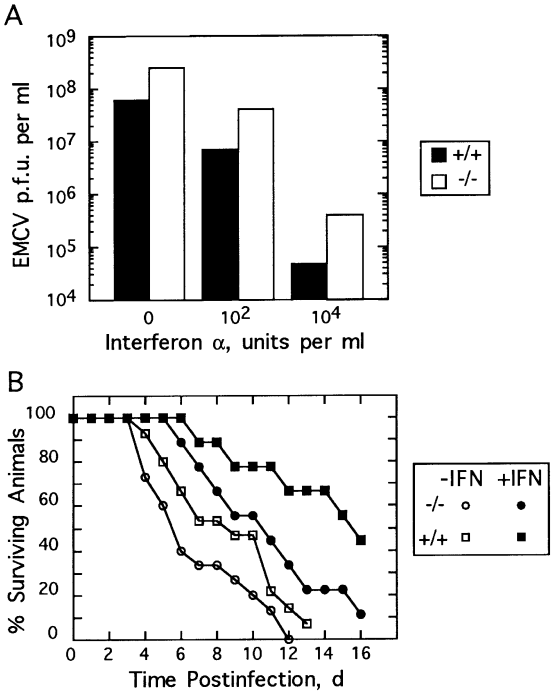

Fig. 3. The anti-EMCV effect of interferon is deficient in RNase $L^{-/-}$ cells and mice. (**A**) The MEF cell lines were incubated in the absence or presence of interferon α for 20 h and infected at an MOI of 0.01 for 14 h prior to harvesting virus. The viral titers as determined by plaque assays on indicator cells are shown. Results are the averages of eight separate infections of cells. (**B**) Survival of mice to EMCV infections in the presence or absence of prior interferon treatment. Mice were injected i.p. with either 500 μl PBS or 10 000 units of interferon α in 500 μl of PBS and 24 h later all mice were injected i.p. with 100 p.f.u. of EMCV in 500 μl of PBS. There were nine interferon treated mice per group and 15 non-interferon treated mice per group.

more efficiently in cells lacking RNase L than in wild type cells, even after interferon treatment, although the effect is relatively small. However, interferon treatment protected the wild type and RNase $L^{-/-}$ primary MEF cells against vesicular stomatitis virus, which is apparently insensitive to the 2-5A system, to the same extent (data not shown).

To extend these findings to animals, survival of mice after intraperitoneal (i.p.) injections of 100 p.f.u. of EMCV was determined (Figure 3B). Even in the absence of interferon treatment, the RNase $L^{-/-}$ mice succumbed to infection before the infected wild type mice. The times, postinfection, required for about half of the mice to die were 5.5 d and 8.5 d for the RNase $L^{-/-}$ and wild type mice, respectively. Effects of interferon α (10^4 units), delivered i.p. one day prior to infection, were determined. The times, postinfection, for about half of the interferon-treated animals to die were 10.5 d and 15.5 d for the RNase $L^{-/-}$ mice and wild type mice, respectively. Therefore, interferon-treatment delayed death by about 5 d and 7 d in the RNase $L^{-/-}$ and wild type mice, respectively. These results show that RNase L contributes to the antiviral mechanism of interferon action in mice. The residual antiviral activity in the interferon-treated, RNase $L^{-/-}$ mice is due to alternative pathways of interferon action (see Discussion).

RNase $L^{-/-}$ mice have enlarged thymuses containing excess numbers of thymocytes

To determine if the absence of RNase L in mice caused any gross or microscopic abnormalities, two week-old wild type and RNase $L^{-/-}$ mice were sacrificed, dissected and the organs examined and compared. The RNase $L^{-/-}$ mice showed remarkably enlarged thymuses (Figure 4A shows representative wild type and RNase $L^{-/-}$ mice). There were no other gross findings nor were there any lesions observed in two week-old RNase $L^{-/-}$ mice. Microscopic and histologic examinations were performed on twenty different tissues. The only obvious finding in the two week-old RNase $L^{-/-}$ mice was the presence in the cortex regions of the thymuses of substantially more cells than in the wild type thymuses (Figure 4B and C). Thymocyte numbers averaged from thirteen of each type of two week-old mice, showed $1.3 \pm 0.21 \times 10^8$ and $2.1 \pm 0.66 \times 10^8$ thymocytes in the wild type and RNase $L^{-/-}$ mice, respectively ($P < 0.0004$). Therefore, the enlarged thymuses resulted from a 1.6-fold increase in the number of thymocytes.

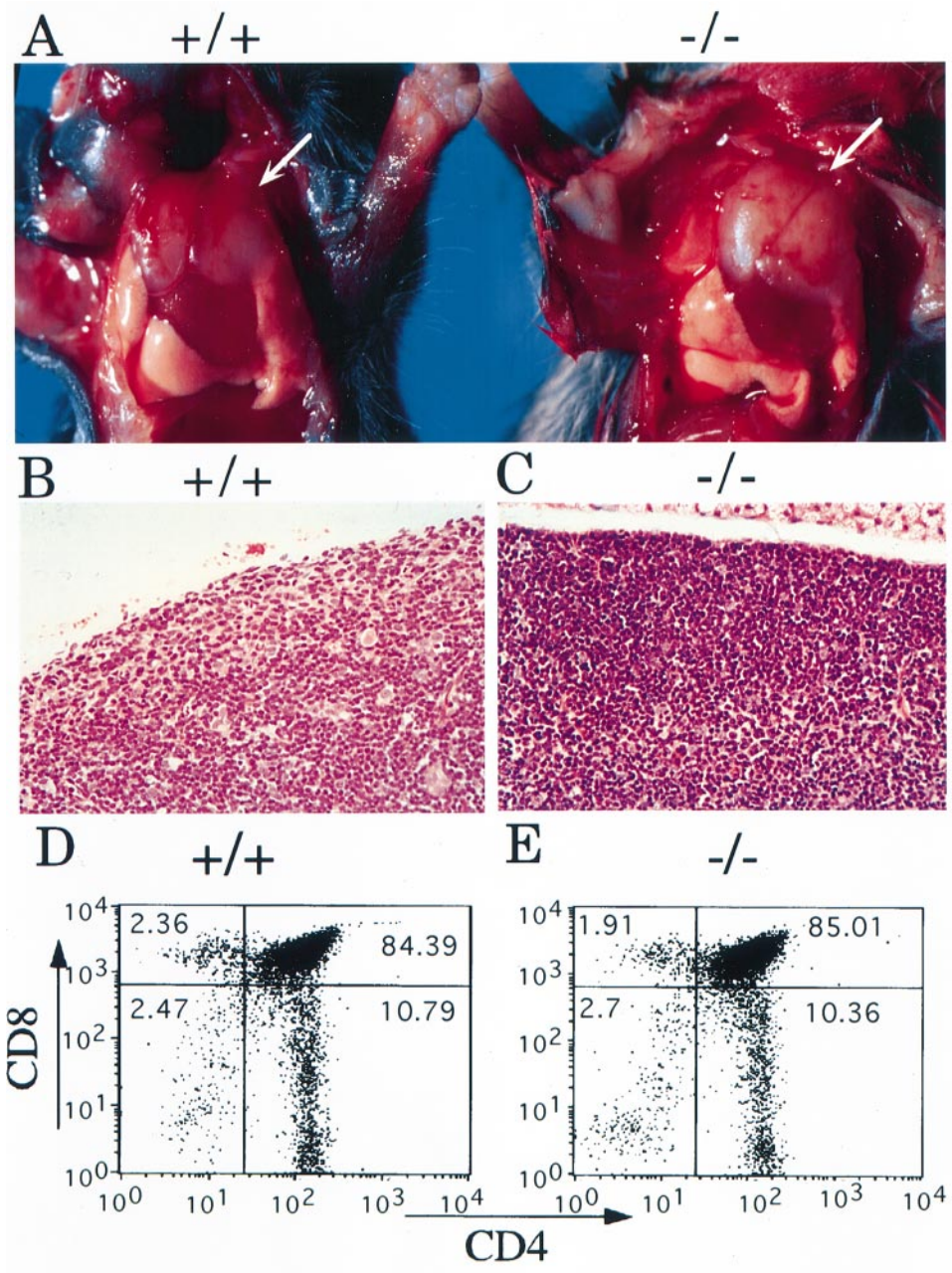

Fig. 4. Enlarged, hypercellular thymuses occur in two week-old RNase $L^{-/-}$ mice. (**A**) Dissected mice show an enlarged thymus in an RNase $L^{-/-}$ mouse. (**B** and **C**) Hematoxlin and eosin stained sections of wild type (+/+) and RNase $L^{-/-}$ thymuses. (**D** and **E**) Thymocyte populations in +/+ and –/– mice. Thymocyte cells from two week-old mice were stained with FITC anti-CD4 and PE anti-CD8 antibodies and were analyzed by flow cytometry. Numbers in each quandrant indicate the percentage of each population in the total thymocyte cell population.

Thymocytes from two week-old RNase $L^{-/-}$ and wild type mice were stained with T cell-specific antibodies and analyzed by flow cytometry to test if a difference in the development of T cell populations accounted for the enlarged thymuses observed in the RNase $L^{-/-}$ mice. Two color analyses indicated no difference in the percentages of double negative ($CD4^-CD8^-$), double positive ($CD4^+CD8^+$) and single positive ($CD4^+CD8^-$ and $CD4^-CD8^+$) populations of thymocytes in the RNase $L^{-/-}$ and wild type mice (Figure 4D and E). In addition, gating and analysis of the individual populations from each of the mice indicated no difference in the expression of TcR (CD3) or the activation antigen CD69 (data not shown).

Reduced levels of apoptosis in the spleen and thymus of RNase $L^{-/-}$ mice

The elevated numbers of thymocytes in the mutant mice could have resulted from increased cell proliferation and/or a failure of cell death. To measure levels of apoptosis in the untreated animals, *in situ* assays for DNA fragmentation were performed on tissue sections from the thymus and spleen (Figure 5). Representative assays from two week-old mice showed substantantially more apoptosis in the wild type thymus than in the RNase $L^{-/-}$ thymus (Figure 5A and B, respectively). Similar findings were obtained in the spleens. Results showed 47% and 57% decreases in the numbers of apoptotic cells in the thymuses and spleens of the RNase $L^{-/-}$ mice compared with wild

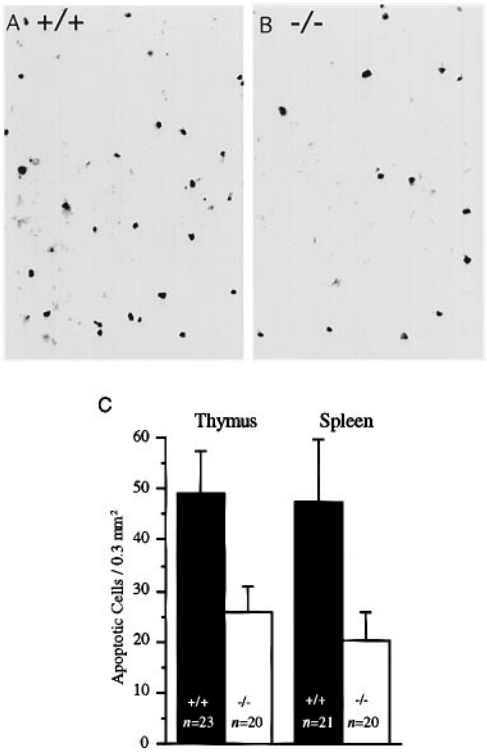

Fig. 5. Reduction in the levels of apoptosis in the thymus and spleen from two week-old RNase L$^{-/-}$ mice. (**A**) ISEL+ stains of thymic specimen from a wild type mouse. (**B**) ISEL+ stains of thymic specimen from an RNase L$^{-/-}$ mouse. (**C**) Average number of apoptotic cells per 0.3 mm^2 of thymic and splenic tissues obtained by using a computer imaging program (NIH Image 1.59) and counting. 5–7 areas of thymus and spleen from each animal were examined and four animals of each type (wild type and RNase L$^{-/-}$) were tested. Vertical bars represent standard deviations. Data was analyzed with two-tail *t*-tests ($P < 0.00001$).

type levels ($P < 0.00001$) (Figure 5C). Therefore, there was a very significant reduction in naturally occurring apoptosis in cells of the spleen and thymus of untreated RNase L$^{-/-}$ mice.

Thymocytes isolated from the mutant mice are resistant to induction of apoptosis

To investigate further the apoptotic defect, thymocytes were isolated and incubated for 4 h with different agents known to induce apoptosis. TUNEL assays for DNA fragmentation were averaged from four to six independent experiments, each performed with thymocytes from different 14- to 17-day-old mice. Remarkably, anti-CD3 treatment of wild type thymocytes resulted in 2.5-fold more apoptotic cells than was obtained by identical treatments of RNase L$^{-/-}$ thymocytes (Figure 6A). In contrast, levels of apoptosis after dexamethasone treatment of the wild type thymocytes was similar to that obtained with mutant thymocytes lacking RNase L. The glucocorticoid-induced pathway of apoptosis, therefore, is not defective in the mutant mice. On the other hand, anti-fas produced 3.8-fold more apoptotic cells when wild type thymocytes were treated in comparison to the identically treated RNase L$^{-/-}$ thymocytes. Similarly, the protein kinase inhibitor, staurosporine, caused 3.1-fold more apoptosis in the wild type thymocytes than in the RNase L$^{-/-}$ thymocytes. Finally, TNFα plus actinomycin D caused 2.3-fold more

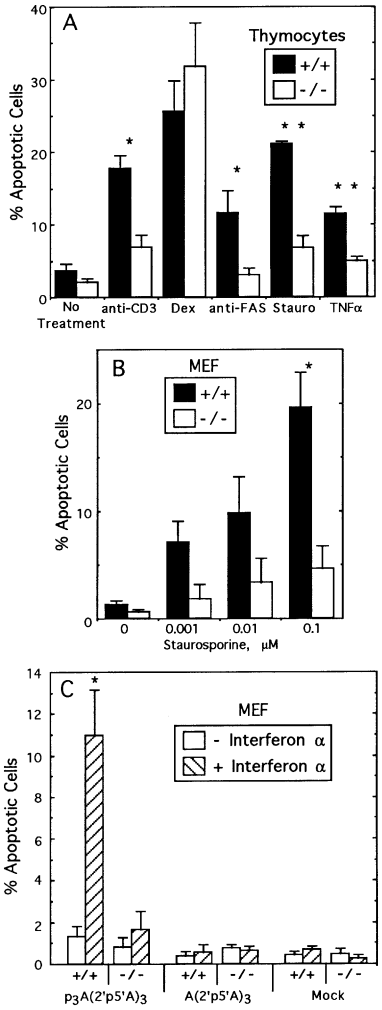

Fig. 6. RNase L$^{-/-}$ thymocytes and MEF cells are resistant to apoptosis. Apoptotic cells were counted after performing TUNEL assays in (**A**) thymocytes and (**B** and **C**) MEF cells treated with various apoptosis inducers (as indicated in the figure). Vertical bars represent standard errors. The data was analyzed with two-tailed *t*-tests (* indicates $P < 0.03$; ** indicates $P < 0.002$). Dex, dexamethasone; stauro, staurosporine.

apoptosis in the wild type thymocytes compared with the RNase L$^{-/-}$ thymocytes (Figure 6A). These results were confirmed by analysis of cytosolic DNA in agarose gels displaying decreased oligonucleosomal laddering in RNase L$^{-/-}$ thymocytes (data not shown).

Annexin V reactivity shows RNase L$^{-/-}$ thymocytes are resistant to apoptosis

During apoptosis, cells gain binding sites for the anticoagulant, annexin V, a calcium-dependent phospholipid binding protein, due to the translocation of phosphatidylserine to the cell surface (Koopman *et al.*, 1994). Therefore, binding sites were monitored on thymocytes by cytofluorimetry with FITC-labeled annexin V (Figure 7). A 2- and 3-fold increase in annexin V binding sites was observed on wild type thymocytes after treatment with anti-CD3 and staurosporine (Figure 7A, B and C). In contrast, there was no increase in annexin V reactivity to similarly treated RNase L$^{-/-}$ thymocytes (Figure 7D, E and F). These results confirm the resistance of RNase L$^{-/-}$ thymocytes to induction of apoptosis by these reagents.

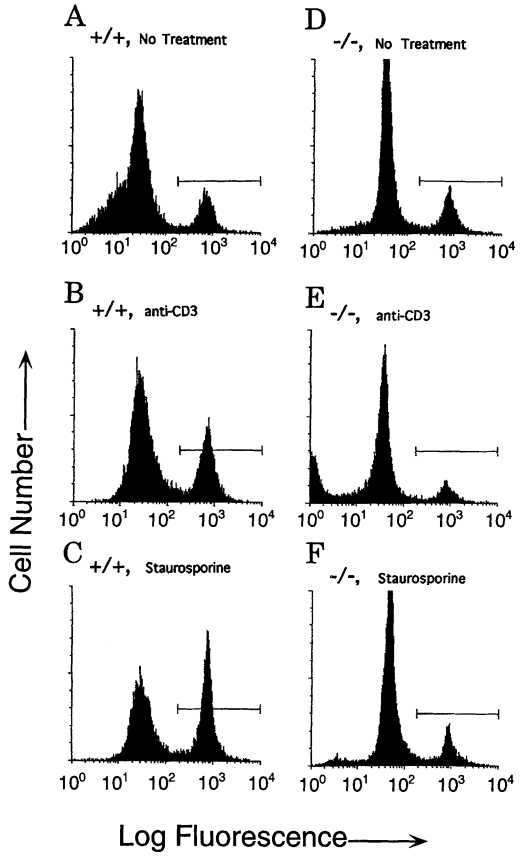

Fig. 7. Annexin V binding assay shows RNase $L^{-/-}$ thymocytes are resistant to induction of apoptosis by anti-CD3 or staurosporine. Flow cytometry analysis for annexin V binding sites in thymocytes from wild type (**A**, **B** and **C**) and RNase $L^{-/-}$ (**D**, **E** and **F**) mice incubated for 4 h with anti-CD3 (B and E) or 4 μM staurosporine (C and F). The horizontal lines indicate apoptotic cells.

Fibroblasts devoid of RNase L are resistant to apoptosis induced by staurosporine or 2-5A

To determine if the defect in apoptosis observed in the thymus and spleen could be extended to other cell types, experiments were performed on fibroblasts (Figure 6B and C). Induction of apoptosis by staurosporine was substantially repressed in the RNase $L^{-/-}$ MEF lines (Figure 6B). Staurosporine (0.1 μM) treatment for 16 h resulted in 3.3-fold more apoptosis in the wild type fibroblasts than in the RNase $L^{-/-}$ fibroblasts. Apoptosis could also be induced by transfection of interferon-treated, wild type MEF cells with $p_3A(2'p5'A)_3$ (Figure 6C). To observe this effect, interferon treatment was necessary, presumably to elevate levels of RNase L. The core 2-5A molecule, $A(2'p5'A)_3$, which is unable to activate RNase L, failed to cause apoptosis in the interferon-treated, wild type cells. In contrast, interferon treatment followed by transfection with functional 2-5A, $p_3A(2'p5'A)_3$, failed to induce apoptosis in the RNase $L^{-/-}$ cells (Figure 6C). These finding show that RNase L activation can lead to apoptosis.

Discussion

RNase L functions in vivo in the antiviral action of the interferon α

Here we provide the first report of a null mutation in a mammalian ribonuclease gene. Mice devoid of RNase L showed a reduced antiviral response to interferon α treatment and a dramatic defect in apoptosis. Therefore, RNase L is likely to play a fundamental role in the control of RNA stability beyond its involvement in interferon action. Previous studies performed in cell culture implicated RNase L in the antiviral activities of the interferons. For example, 2-5A or related material and/or characteristic rRNA cleavages occur in interferon-treated, mammalian cells after infection with EMCV, vaccinia virus, reovirus, herpes simplex virus (HSV) and SV40 (reviewed in Silverman and Cirino, 1997). In addition, expression of 2-5A synthetase cDNA restricted replication of EMCV, mengo virus and HIV-1 while a dominant-negative RNase L suppressed the anti-EMCV effect of interferon (Chebath *et al.*, 1987b; Rysiecki *et al.*, 1989; Schroder *et al.*, 1990; Hassel *et al.*, 1993). However, experiments performed with the RNase $L^{-/-}$ mice provide the first evidence that the 2-5A system functions as antiviral pathway *in vivo* (Figure 3). The average survival time after EMCV infection was decreased by 3 days in the RNase $L^{-/-}$ mice (Figure 3B). Furthermore, while interferon treatment extended survival of both the RNase $L^{-/-}$ and wild type mice, death occurred about 5 days earlier in the mice lacking RNase L.

The residual, antiviral activity of interferon in the RNase $L^{-/-}$ mice is due to alternative antiviral pathways. Multiple antiviral pathways probably evolved to ensure the survival of species from viruses capable of evading one or more host defense mechanism. For example, interferon-treated, HSV-infected cells accumulate 2-5A analogs that block RNase L activation and EMCV-infection of non-interferon treated cells leads to the inactivation of RNase L (Cayley *et al.*, 1982, 1984). Alternative antiviral mechanisms of interferon action include the dsRNA-dependent protein kinase PKR, Mx proteins, and probably other pathways (Pavlovic and Staeheli, 1991; Williams, 1995). $PKR^{-/-}$ mice are defective for the anti-EMCV activities of interferon γ and dsRNA but not of interferon α (Yang *et al.*, 1995). However, because of differences in the protocols between that study and the one used here, including much higher doses of EMCV and interferon in Yang *et al.* (1995), it is difficult to compare results. Some contribution of PKR to the interferon α effect against EMCV seems likely based on previous studies (Meurs *et al.*, 1992). A further interesting parallel between the PKR and 2-5A systems is that both pathways contribute to apoptosis. PKR functions in stress-mediated apoptosis in response to dsRNA, TNF-α or LPS by inducing interferon regulatory factor 1 (IRF-1) DNA binding activity and Fas mRNA (Der *et al.*, 1997). Interestingly, $IRF\text{-}1^{-/-}$ T lymphocytes are resistant to DNA damaged-induced apoptosis (Tamura *et al.*, 1995).

Involvement of RNase L in thymus development and the control of cell death

A null mutation in the gene for the essential apoptotic factor, caspase-3 (CPP-32), is lethal, while mice with disruptions of the caspase-1 (ICE) gene, appear normal (Li *et al.*, 1995; Kuida *et al.*, 1995, 1996). RNase $L^{-/-}$ mice have a phenotype which is intermediate between these two extremes. While the possible long term effects of the absence of RNase L in mice is under investigation, in 2- to 3-week-old mice there were dramatically enlarged thymuses containing significantly increased numbers of thymocytes compared with wild type mice. The enlarged thymuses can be explained by the

reduced ability of thymocytes to undergo apoptosis (Figures 5–7). RNase $L^{-/-}$ thymocytes were resistant to induction of apoptosis by anti-CD3, anti-fas, staurosporine and TNF-α. However, induction of apoptosis by dexamethasone was unimpaired in the RNase $L^{-/-}$ thymocytes (Figure 6A). In the activation-induced death of T cells, TCR/CD3 crosslinking induces expression of fas and fas ligand which leads to apoptosis (Brunner *et al.*, 1995; Ju *et al.*, 1995). Therefore, the apoptotic defect in the RNase $L^{-/-}$ thymocytes is downstream of fas. TNF-α induces separate apoptotic signals involving caspase-8 (FLICE/MACH) and a RIP kinase while staurosporine is a general inducer of apoptosis that inhibits protein kinases (Jacobson *et al.*, 1994; Nagata, 1997).

The apoptotic defect in the RNase $L^{-/-}$ mice was observed in thymocytes, embryonic fibroblasts and in the spleen (Figure 5–7). Cell lines that express an RNase L dominant-negative mutant are also resistant to induction of apoptosis by various agents (J.Castelli, B.Hassel, J.Paranjape, R.H.Silverman and R.Youle, in preparation). Therefore, the absence of RNase L has an anti-apoptotic effect in multiple cell types treated with a variety of different agents. Because interferon treatment causes induction of 2-5A-synthetase and RNase L, it is possible that the 2-5A system also contributes to the pro-apoptotic effects of interferon (Sangfelt *et al.*, 1997). Introducing 2-5A into interferon-treated, wild type fibroblasts causes apoptosis while failing to cause death of interferon-treated, RNase $L^{-/-}$ cells, suggesting that RNase L activation can lead to apoptosis (Figure 6C).

The apoptotic defects in the RNase $L^{-/-}$ mice are presumably due to a reduced ability to degrade certain RNA molecules. The cellular dsRNA activators of 2-5A synthetases could be formed during the condensation and degeneration of the cell nucleus. For instance, highly structured RNA from the decay of nuclear ribonucleoprotein complexes might become available for activation of 2-5A synthetases. RNase L could contribute to apoptosis by degrading mRNAs for anti-apoptotic factors or cell survival factors. In the absence of RNase L, therefore, such cell survival factors would accumulate to higher levels than in wild type cells. Alternatively, RNase L could be involved in processing pro-apoptotic (death) factor mRNAs, thus maintaining levels of these protein. Another possibility is that RNase L could be a component of the enzymatic machinery that catalyzes the autodegradation of the cells. For example, rRNA degradation occurs during apoptosis in response to different chemical inducers (Houge *et al.*, 1995). Decay of rRNA by RNase L could indirectly lead to apoptosis by inhibiting protein synthesis.

Host defenses against viruses may include sacrificing infected cells through a unique oligonucleotide-mediated signal to RNase L

The highly selective interaction of 2-5A with RNase L provides an unambiguous signal for the induction of RNA cleavages. The uniqueness of the 2-5A binding domain in RNase L is underscored by the absence of proteins that can be crosslinked to a 2-5A probe in several different organs of the RNase $L^{-/-}$ mice (Figure 2A). Because RNase L is encoded by a single gene, the homozygous disruption of the RNase L gene is also a knockout of the 2-5A system *per se*. In contrast, because the 2-5A synthetases are encoded by multiple genes it would have been considerably more difficult to ablate the 2-5A system by targeting these genes (Rutherford *et al.*, 1991).

It is no coincidence that an antiviral pathway of interferon action functions in apoptosis. Apoptosis is a basic response of cells to many different types of virus infections. Viruses have responded to this challenge by evolving genes encoding an impressive array of anti-apoptosis factors (Vaux and Strasser, 1996). In essence, viruses ensure their own survival by blocking the ability of host cells to undergo apoptosis. The results of this study provide the surprising finding that RNase L is a death factor which probably contributes to the antiviral activity of interferon by eliminating infected cells. While the molecular events responsible for the pro-apoptotic activity of RNase L are currently unknown, the RNase $L^{-/-}$ mice are an indispensable resource for the discovery of the *in vivo* RNA substrates of RNase L.

Materials and methods

Construction of the RNase L gene targeting vector and homologous recombination in murine embryonic stem cells

Genomic clones for murine RNase L were isolated from a lambda dash phage library of mouse strain 129 DNA (a gift of T.Doetschman, Cincinnati) by screening with a ^{32}P-labeled murine RNase L cDNA probe. A *neo* gene isolated from plasmid pmc1*neo*polyA (Stratagene Co.) was inserted in reverse orientation into a *Bam*H1 site in the first coding exon of the RNase L gene and a herpes simplex virus thymidine kinase (TK) gene was fused to the 5′ end of the gene fragment (Figure 1). ES cells (line E14.1) (a kind gift from W.Muller) from mouse strain 129/ola were cultured on feeder layers of embryonic fibroblasts treated with mitomycin C (10 μg/ml) in medium containing leukemia inhibitory factor, LIF (1000 units/ml). The *Kpn*I linearized targeting construct was electroporated into the ES cells. Cells were selected on the feeder layers in the presence of both G418 (200 μg/ml) and ganciclovir (650 ng/ml). Drug resistant clones were obtained 8 to 10 days later and were propagated and divided for storage in liquid nitrogen. Two cell lines, AZ3 and AZ16, were identified by Southern blot analysis to contain a disruption of the RNase L gene due to homologous recombination with the targeting vector.

Generation of RNase $L^{-/-}$ mice

The AZ3 and AZ16 ES cells were injected into C57Bl6 mouse blastocysts and implanted into foster mothers resulting in several chimeric offspring mice, however, only the AZ16 cells led to the generation of mice with the mutated RNase L gene in the germ line (embryo injections and implantations were performed by J.Duffy, The University of Cincinnati ES Cell/Mouse Service Core Laboratories). These mice were bred and tail DNA from the offspring was analyzed in Southern blots to determine germ line transmissibility (Figure 1). The DNA preparations isolated from the mouse tails were digested with *Xba*I and used to prepare Southern blots. Two ^{32}P-labeled DNA probes were used, one was a *Hin*dIII/*Hin*dIII fragment of the murine RNase L gene (indicated in Figure 1A) and the other was from the *neo* gene. Heterozygous mice were intercrossed to obtain a RNase $L^{-/-}$ mice.

Preparation and culture of primary mouse embryonic fibroblasts (MEF)

Heterozygous mice were intercrossed and MEFs were prepared from the resulting embryos at day 16.5 post-coitum. Individual sibling embryos were removed, while maintaining sterility, to tissue culture dishes containing PBS. The embryos were minced and pieces of tissue were removed for genotyping by Southern blot analysis. The remaining tissue was incubated at 4°C for 16 h with 0.05% trypsin and 0.53 mM EDTA. The excess trypsin solution was then aspirated and discarded and the tissue was incubated at 37°C for 30 min. Two volumes of DMEM containing 10% FBS was added followed by vigorous pipetting to break up the tissue into cells. The cells were then cultured in fresh DMEM/10%FBS. Cell lines were derived by continuous culturing for 10 to 14 passages to obtain immortalized cells.

Immunodetection of RNase L in Western blots

A polyclonal antibody against a fragment of murine RNase L (amino acid residues 99–616) was prepared for detection of RNase L on Western blots. A 1551 bp fragment of murine RNase L cDNA, obtained by digesting plasmid pZB1 (Zhou *et al.*, 1993) with *Bam*HI and *Pst*I, was subcloned into plasmid pQE (Qiagen) and expressed in *E.coli* XL1 Blue (Stratagene). The insoluble, expressed protein was purified and injected into rabbit (Duncroft Assoc.). Nonspecific antibodies were removed by three successive incubations of the antiserum with resuspended pellets of XL1 Blue cell lysate followed by centrifugation at 12 400 *g* for 60 min at 4°C to remove pelleted material.

2-5A binding assay for RNase L

The ^{32}P-labeled and bromine substituted 2-5A analog, $p(A2'p)_2$-$(br^8A2'p)_2A[^{32}P]Cp$, was covalently crosslinked to RNase L in crude extracts of mice organs as described previously (Nolan-Sorden *et al.*, 1990). Briefly, 10^5 c.p.m. (at 3000 Ci/mmole) of 2-5A probe was incubated for 1 h on ice with 200 μg of tissue extract prepared as described (Silverman and Krause, 1987). Covalent crosslinking was done under an ultraviolet lamp (308 nm) for 1 h on ice and the proteins were separated on SDS–10% polyacrylamide gels.

Assay for ribonuclease activity with 18S rRNA as substrate

MEF cells at about 75% confluency in 100 mm dishes were incubated with 1000 units/ml hybrid recombinant human interferon-α BDBB (a gift from H.-K.Hochkeppel, Novartis Pharma AG) (Gangemi *et al.*, 1989) for 16 h. This type of interferon is active on both human and murine cells and was used in all experiments involving added interferon. Cells were incubated for 1 h with fresh media plus serum, washed with Optimem (Gibco/BRL), and either mock transfected or transfected with 5 μM $A(2'p5'A)_2$ (Sigma) or $p_3A(2'p5'A)_2$ by calcium phosphate coprecipitation (Hovanessian *et al.*, 1979). [The $p_3A(2'p5'A)_2$ was prepared with human 2-5A synthetase as described (Silverman and Krause, 1987)]. Incubation of cells with calcium phosphate precipitates was for 60 min, after which cells were washed, fresh medium added and incubated for an additional 90 min before harvesting. Total RNA, 20 μg per assay, was isolated using the RNazol reagent (TelTest). RNA was separated on 1.2% formaldehyde gels, transferred to Nytran membrane (Schleicher & Schuell) and hybridized to a ^{32}P-labeled human 18S rRNA cDNA (American Type Culture Collection).

Assays for the antiviral activity of interferon

EMCV (American Type Culture Collection) was grown in murine L929 cells and the viral titers determined by plaque assays on murine L929 cells. MEF cell lines were incubated for 20 h in the presence or absence of interferon α prior to infections. EMCV at an MOI of 0.01 in DMEM containing 2% fetal bovine serum was added to the cells and incubated 1 h to allow the virus to adsorb to the cells. The medium was replaced with DMEM containing 10% fetal bovine serum. At 14 h post-infection, virus was harvested and titered by plaque assays on murine L929 cells.

Five-week-old mice (wild type and RNase $L^{-/-}$) were either untreated or injected i.p. with 10^4 units of interferon α at 20 h prior to infections. Subsequently, mice were injected i.p. with 100 p.f.u. of EMCV and monitored daily for survival.

Monitoring apoptosis in vivo

Apoptosis in the thymuses and spleens of 14-day-old mice was analyzed by the *in situ* DNA end-labeling plus (ISEL+) method with digoxigenin-11-dUTP and terminal deoxynucleotidyl transferase (Blaschke *et al.*, 1996). Alkaline phosphatase-conjugated anti-digoxigenin Fab fragments binding to the labeled DNA was detected by enzymatic reaction using nitroblue tetrazolium (NBT) and 5-bromo-4-chloro-3-indolyl phosphate (BCIP) as substrates, giving a blue precipitate.

Preparation, culture and treatment of thymocytes

Mice, aged 14–17 day-old, were sacrificed, dissected and the thymuses were removed. Thymocytes isolated using a 70 μm cell strainer (Falcon) were diluted in medium, DMEM (Gibco/BRL), 1 mg/ml of bovine serum albumin (Sigma), 15 mM HEPES (pH 7.4). Viable cell numbers were determined by Trypan blue dye exclusion assay with a hemocytometer and are expressed ± standard deviation. Thymocytes were incubated at 2×10^6 cells/ml in six-well plates. Apoptosis of thymocytes was induced by treatment with 4 μM staursporine (Sigma), 1 μM dexamethasone (Sigma), 50 ng/ml of rabbit polyclonal antibody to human fas (Ab-1) (Calbiochem) or a combination of 1 ng/ml murine TNF α (Boehringer Mannheim) and 50 ng/ml actinomycin D (Sigma). In addition, apoptosis of thymocytes was induced on plate wells coated with 20 μg/ml monoclonal rat anti-murine CD3 (Deveron Chemicals) for 4 h prior to use. Incubation of thymocytes in the presence or absence of apoptosis inducers was for 4 h at 37°C.

Flow cytometric analysis of thymocytes

Two and three color flow cytometry was performed using standard methods. Briefly, single cell suspensions from thymuses were prepared and 1 to 2×10^6 cell aliquots were washed twice with staining buffer (Dulbecco's PBS with 2% FCS, 0.2% NaN_3). The cells were incubated on ice in 100 μl rat serum (Rockland Inc., Gilbertsville, PA) diluted 1:1000 in the staining buffer. After 20 min, the cells were washed twice, resuspended in 200 μl of staining buffer, and stained with FITC-anti-CD4, PE-anti-CD8 and CY-anti-CD3e antibodies (Pharmingen, San Diego, CA). After 30 min, the cells were washed 5 times, resuspended in staining buffer and analyzed by two and three color flow cytometry using a FACScan™ (Becton-Dickinson, San Jose, CA). In some experiments, aliquots of thymocytes were stained with CY-anti-CD3e and PE-conjugated anti-CD4 or anti-CD8 antibodies. After washing, the cells were stained with FITC-annexin V (R & D Systems, Minneapolis, MN) and analyzed by three color cytometry. Sample data were collected on 20 000 ungated cells. Individual cell populations were gated and analyzed using CellQuest™ (Becton Dickinson).

TUNEL assays for DNA fragmentation in cultured cells

Thymocytes incubated in the presence or absence of apoptosis inducers were spread on polylysine coated slides (Sigma), fixed and washed. Assays for DNA fragmentation by the TUNEL method was performed with FITC-labeled dUTP and terminal deoxynucleotidyl transferase as described by the supplier of the reagents (Promega) (Gavrieli *et al.*, 1992). Cells were observed under a fluorescence microscope (Nikon Microphot FXA) and results expressed as the percentages of apoptotic cells ± standard errors.

Apoptosis assay by Annexin V binding

Annexin V-FITC conjugate and flow cytometry was used to detect phosphatidylserine on the cell surface (an early feature of apoptotic cells). Assay were performed as described (Bender Medsystems). Briefly, 2×10^5 thymocytes per assay were centrifuged [2,000×g for 5 min at 2°C], washed in PBS and resuspended in binding buffer [10 mM HEPES pH 7.4, 140 mM NaCl and 2.5 mM $CaCl_2$]. Cells were incubated with 1 μg/ml annexin V-FITC conjugate and 0.5 μg/ml propidium iodide in the dark at 37°C for 15 min and then centrifuged, washed and resuspended in binding buffer. Cells were analyzed by two color cytometry using a FACScanTM (Becton-Dickinson, San Jose, CA). Sample data was collected on 20 000 ungated cells and apoptotic versus necrotic cells were separated and analyzed using CellQuestTM (Becton Dickinson).

Induction of apoptosis in MEFs

MEFs were grown on chamber slides (Lab-Tek) to 70–80% confluency and were treated with varying concentrations of staurosporine overnight. Alternately, MEFs on slides were incubated with or without 1000 units/ml interferon α for 16 to 18 h and mock transfected or transfected with 5 μM $A(2'p5'A)_2$ (Sigma) or 5 μM $p_3A(2'p5'A)_2$ by calcium phosphate coprecipitation (Hovanessian *et al.*, 1979). The transfection protocol was as described above except after washing, cells were incubated 16 h at 37°C. Cells were washed with PBS and fixed in 4% paraformaldehyde on ice for 25 to 30 min, washed in PBS and stored at –20°C in 70% ethanol. Apoptosis was monitored by TUNEL assays as described above.

Acknowledgements

The interferon was a generous gift of H.-K.Hochkeppel (Norvatis Pharma AG) and the 2-5A analog was generously provided by P.F.Torrence (Bethesda). We thank T.Doetschman and J.Duffy (Cincinnati) for their expertise, R.Youle (Bethesda), G.Stark and B.Williams (Cleveland) for advice, A.Raber for flow cytometry, A.Allen (Microbiological Associates, Rockville, MD) for histology, and J.Lang for expert photography. Support was by US National Cancer Institute Grant CA44059 to R.H.S.

References

Blaschke,A.J., Staley,K. and Chun,J. (1996) Widespread programmed cell death in proliferative and postmitotic regions of the fetal cerebral cortex. *Development*, **122**, 1165–1174.

Brunner,T. *et al.* (1995) Cell-autonomous Fas (CD95)/Fas-ligand interaction mediates activation-induced apoptosis in T-cell hybridomas. *Nature*, **373**, 441–444.

Cayley,P.J., Knight,M. and Kerr,I.M. (1982) Virus-mediated inhibition of the ppp(A2′p)$_n$A system and its prevention by interferon. *Biochem. Biophys. Res. Commun.*, **104**, 376–382.

Cayley,P.J., Davies,J.A., McCullagh,K.G. and Kerr,I.M. (1984) Activation of the ppp(A2′p)nA system in interferon-treated, herpes simplex virus-infected cells and evidence for novel inhibitors of the ppp(A2′p)$_n$A-dependent RNase. *Eur. J. Biochem.*, **143**, 165–174.

Chebath,J., Benech,P., Hovanessian,A., Galabru,J. and Revel,M. (1987a) Four different forms of interferon-treated 2′,5′-oligo(A) synthetase identified by immunoblotting in human cells. *J. Biol. Chem.*, **262**, 3852–3857.

Chebath,J., Benech,P., Revel,M. and Vigneron,M. (1987b) Constitutive expression of (2′-5) oligo A synthetase confers resistance to picornavirus infection. *Nature*, **330**, 587–588.

Cohrs,R.J., Goswami,B.B. and Sharma,O.K. (1988) Occurrence of 2-5A and RNA degradation in the chick oviduct during rapid estrogen withdrawal. *Biochemistry*, **27**, 3246–3252.

Cole,J., Carroll,S.S. and Kuo,L.C. (1996) Stoichiometry of 2′,5′-oligoadenylate-induced dimerization of ribonuclease L. A sedimentation equilibrium study. *J. Biol. Chem.*, **271**, 3979–3981.

Der,S.D., Yang,Y.-L., Weissmann,C. and Williams,B.R.G. (1997) A PKR-dependent pathway mediating stress-induced apoptosis. *Proc. Natl Acad. Sci. USA*, **94**, 3279–3283.

Dong,B. and Silverman,R.H. (1995) 2-5A-dependent RNase molecules dimerize during activation by 2-5A. *J. Biol. Chem.*, **270**, 4133–4137.

Dong,B. and Silverman,R.H. (1997) A bipartite structure of 2-5A dependent RNase L. *J. Biol. Chem.*, **272**, 22236–22242.

Dong,B., Xu,L., Zhou,A., Hassel,B.A., Lee,X., Torrence,P.F. and Silverman,R.H. (1994) Intrinsic molecular activities of the interferon-induced 2-5A-dependent RNase. *J. Biol. Chem.*, **269**, 14153–14158.

Gangemi,J.D., Lazdins,J., Dietrich,F.M., Matter,A., Poncioni,B. and Hochkeppel,H.K. (1989) Antiviral activity of a novel recombinant human interferon-alpha B/D hybrid. *J. Interferon Res.*, **9**, 227–237.

Gavrieli,Y., Sherman,Y. and Ben-Sasson,S.A. (1992) Identification of programmed cell death *in situ* via specific labeling of nuclear DNA fragmentation. *J. Cell Biol.*, **119**, 493–501.

Hassel,B.A., Zhou,A., Sotomayor,C., Maran,A. and Silverman,R.H. (1993) A dominant-negative mutant of 2-5A-dependent RNase suppresses antiproliferative and antiviral effects of interferon. *EMBO J.*, **12**, 3297–3304.

Houge,G., Robaye,B., Eikhom,T.S., Golstein,J., Mellgren,G., Gjertsen, B.T., Lanotte,M. and Doskeland,S.O. (1995) Fine mapping of 28S rRNA sites specifically cleaved in cells undergoing apoptosis. *Mol. Cell. Biol.*, **15**, 2051–2062.

Hovanessian,A.G., Brown,R.E. and Kerr,I.M. (1977) Synthesis of low molecular weight inhibitor of protein synthesis with enzyme from interferon-treated cells. *Nature*, **268**, 537–539.

Hovanessian,A.G., Wood,J., Meurs,E. and Montagnier,L. (1979) Increased nuclease activity in cells treated with pppA2′p5′A2′p5′A. *Proc. Natl Acad. Sci. USA*, **76**, 3261–3265.

Jacobsen,H., Czarniecki,C.W., Krause,D., Friedman,R.M. and Silverman,R.H. (1983) Interferon-induced synthesis of 2-5A-dependent RNase in mouse JLS-V9R cells. *Virology*, **125**, 496–501.

Jacobson,M.D., Burne,J.F. and Raff,M.C. (1994) Programmed cell death and bcl-2 protection in the absence of a nucleus. *EMBO J.*, **13**, 1899–1994.

Ju,S.T., Panka,D.J., Cui,H., Ettinger,R., el-Khatib,M., Sherr,D.H., Stanger,B.Z. and Marshak-Rothstein,A. (1995) Fas(CD95)/FasL interactions required for programmed cell death after T-cell activation. *Nature*, **373**, 444–448.

Kerr,I.M. and Brown,R.E. (1978) pppA2′p5′A2′p5′A: An inhibitor of protein synthesis synthesized with an enzyme fraction from interferon-treated cells. *Proc. Natl Acad. Sci. USA*, **75**, 256–260.

Koopman,G., Reutelingsperger,C.P.M., Kuijten,G.A.M., Keehnen, R.M.J., Pals,S.T. and van Oers,M.H.J. (1994) Annexin V for flow cytometric detection of phosphatidylserine expression on B cells undergoing apoptosis. *Blood*, **84**, 1415–1420.

Kuida,K., Lippke,J.A., Ku,G., Harding,M.W., Livingston,D.J., Su,M.S.-S. and Flavell,R.A. (1995) Altered cytokine export and apoptosis in mice deficient in interleukin-1β converting enzyme. *Science*, **267**, 2000–2003.

Kuida,K., Zheng,T.S., Na,S., Kuan,C.-y., Yang,D., Karasuyama,H., Rakic,P. and Flavell,R.A. (1996) Decreased apoptosis in the brain and premature lethality in CPP-32-deficient mice. *Nature*, **384**, 368–375.

Li, P. *et al.* (1995) Mice deficient in IL-1β-converting enzyme are defective in production of mature IL-1β and resistant to endotoxic shock. *Cell*, **80**, 401–411.

Meurs,E.F., Watanabe,Y., Kadereit,S., Barber,G.N., Katze,M.G., Chong,K., Williams,B.R.G. and Hovanessian,A.G. (1992) Constitutive expression of human double-stranded RNA-activated p68 kinase in murine cells mediates phosphorylation of eukaryotic initiation factor 2 and partial resistance to encephalomyocarditis virus growth. *J. Virol.*, **66**, 5805–5814.

Nagata,S. (1997) Apoptosis by death factor. *Cell*, **88**, 355–365.

Nolan-Sorden,N.L., Lesiak,K., Bayard,B., Torrence,P.F. and Silverman,R.H. (1990) Photochemical crosslinking in oligonucleotide-protein complexes between a bromine-substituted 2-5A analogue and 2-5A-dependent RNase by ultraviolet lamp or laser. *Anal. Biochem.*, **184**, 298–304.

Pavlovic,J. and Staeheli,P. (1991) The antiviral potentials of Mx proteins. *J. Interferon Res.*, **11**, 215–219.

Reid,T.R., Hersh,C.L., Kerr,I.M. and Stark,G.R. (1984) Analysis of 2′,5′-oligoadenylates in cells and tissues. *Anal. Biochem.*, **136**, 136–141.

Rutherford,M.N., Kumar,A., Nissim,A., Chebath,J. and Williams,B.R.G. (1991) The murine 2-5A synthetase locus: three distinct transcripts from two linked genes. *Nucleic Acids Res.*, **19**, 1917–1924.

Rysiecki,G., Gewert,D.R. and Williams,B.R.G. (1989) Constitutive expression of a 2′,5′-oligoadenylate synthetase cDNA results in increased antiviral activity and growth suppression. *J. Interferon Res.*, **9**, 649–657.

Sangfelt,O., Erickson,S., Castro,J., Heiden,T., Einhorn,S. and Grander,D. (1997) Induction of apoptosis and inhibition of cell growth are independent responses to interferon-α in hematopoietic cell lines. *Cell Growth Differ.*, **8**, 343–352.

Schroder,H.C., Ugarkovic,D., Merz,H., Kuchino,Y., Okamoto,T. and Muller,W.E.G. (1990) Protection of HeLa-T4+ cells against human immunodeficiency virus (HIV) infection after stable transfection with HIV LTR-2′,5′-oligoadenylate synthetase hybrid gene. *FASEB J.*, **4**, 3124–3130.

Silverman,R.H. (1997) 2-5A dependent RNase L: a regulated endoribonuclease in the interferon system. In D'Alessio,G. and Riordan,J.F. (eds), *Ribonucleases: Structure and Functions*. Academic Press, New York, pp. 515–551.

Silverman,R.H. and Krause,D. (1987) Interferon-regulated 2-5A- and protein kinase systems. In Clemens,M.J., Morris,A.G. and Gearing,A.J.H. (eds), *Lymphokines and Interferons: A Practical Approach*. IRL Press, Oxford, UK, pp. 149–193.

Silverman,R.H. and Cirino,N.M. (1997) RNA decay by the interferon regulated 2-5A system as a host defense against viruses. In Morris,D.R. and Harford,J.B. (eds.), *mRNA Metabolism and Post-Transcriptional Gene Regulation*. John Wiley & Sons, New York, pp. 295–309.

Silverman,R.H., Skehel,J.J., James,T.C., Wreschner,D.H. and Kerr,I.M. (1983) rRNA Cleavage as an index of ppp(A2′p)$_n$A activity in interferon-treated encephalomyocarditis virus-infected cells. *J. Virol.*, **46**, 1051–1055.

Stark,G.R., Dower,W.J., Schimke,R.T., Brown,R.E. and Kerr,I.M. (1979) 2-5A synthetase: assay, distribution and variation with growth or hormone status. *Nature*, **278**, 471–473.

Tamura,T. *et al.* (1995) An IRF-1-dependent pathway of DNA damage-induced apoptosis in mitogen-activated T lymphocytes. *Nature*, **376**, 596–599.

Vaux,D.L. and Strasser,A. (1996) The molecular biology of apoptosis. *Proc. Natl Acad. Sci. USA*, **93**, 2239–2244.

Williams,B.R.G. (1995) The role of the dsRNA-activated kinase, PKR, in signal transduction. *Seminars in Virology*, **6**, 191–202.

Williams,B.R.G., Golgher,R.R., Brown,R.E., Gilbert,C.S. and Kerr,I.M. (1979) Natural occurrence of 2-5A in interferon-treated EMC virus-infected L cells. *Nature*, **282**, 582–586.

Wreschner,D.H., James,T.C., Silverman,R.H., Kerr,I.M. (1981) Ribosomal RNA cleavage, nuclease activation and 2-5A(ppp(A2′p)$_n$A) in interferon-treated cells. *Nucleic Acids Res.*, **9**, 1571–1581.

Yang,Y.-L., Reis,L.F.L., Pavlovic,J., Aguzzi,A., Schafer,R., Kumar,A., Williams,B.R.G., Aguet,M. and Weissmann,C. (1995) Deficient signaling in mice devoid of double-stranded RNA-dependent protein kinase. *EMBO J.*, **14**, 6095–6106.

Zhou,A., Hassel,B.A. and Silverman,R.H. (1993) Expression cloning of 2-5A-dependent RNAase: A uniquely regulated mediator of interferon action. *Cell*, **72**, 753–765.

Received on July 16, 1997; revised on August 22, 1997